Robotica (2023), **41**, pp. 3116–3136
doi:10.1017/S0263574723000905

CAMBRIDGE UNIVERSITY PRESS

RESEARCH ARTICLE

Path tracking control method for automatic navigation rice transplanters based on VUFC and improved BAS algorithm

Dequan Zhu[1,2], Menghao Shi[1], Yang Wang[1], Kang Xue[1], Juan Liao[1], Wei Xiong[1], Fuming Kuang[1] and Shun Zhang[1]

[1]School of Engineering, Anhui Agricultural University, Hefei, P.R. China and [2]Anhui Province Engineering Laboratory of Intelligent Agricultural Machinery Equipment, Anhui Agricultural University, Hefei, China
Corresponding author: Dequan Zhu; Email: zhudequan@ahau.edu.cn

Received: 23 March 2023; **Revised:** 24 May 2023; **Accepted:** 10 June 2023; **First published online:** 10 July 2023

Keywords: path tracking algorithm; pure pursuit algorithm; rice transplanter; the beetle antennae search algorithm; variable universe fuzzy control

Abstract

During the operation of automatic navigation rice transplanter, the accuracy of path tracking is influenced by whether the transplanter can enter the stable state of linear path tracking quickly, thus affecting the operation quality and efficiency. To reduce the time to enter the path tracking stable state and improve the tracking accuracy and stability for the rice transplanter, path tracking control method based on variable universe fuzzy control (VUFC) and improved beetle antenna search (BAS) is proposed in this paper. VUFC is applied to achieve adaptive adjustment of the fuzzy universe by dynamically adjusting the quantization and scaling factors according to the variations of errors by the contraction–expansion factor. To solve the problem of setting the contraction–expansion factor in VUFC and real-time performance, an offline parameter optimization method is presented to calculate the optimal contraction–expansion factor by an iterative optimization algorithm in a path tracking simulation model, where the iterative optimization algorithm is the BAS algorithm improved by the isolated niching technique and adaptive step size strategy in this paper. To verify the effectiveness of the proposed path tracking control method, simulation and field linear path tracking experiments were carried out. Experimental results indicate that the proposed method reduces the time of entering the stable state of linear path tracking and improves the accuracy and stability of path tracking compared with the pure pursuit control method.

1. Introduction

With the development of precision agriculture, automatic navigation of agricultural machinery has been widely used in arming, sowing, fertilization, spraying, harvesting, and other agricultural production processes [1, 2]. Accurate acquisition of position information and lateral control method directly affect the performance of agricultural machinery automatic navigation [3]. Due to the complex paddy field environment and uneven pavement, the operation of automatically driving rice transplanter into the straight tracking state is frequent and difficult [4]. Therefore, to improve the operation quality and efficiency of the automatic navigation rice transplanter, it is necessary to optimize the rise time and overshoot of linear path in the path tracking control process of rice transplanter, as to meet the requirements of short time to enter the stable state of linear path tracking, high accuracy of path tracking, and strong resistance to interference in the complex paddy field environment.

Thus far, lots of studies on path tracking control methods for agricultural machinery navigation have been introduced. Most of them constructed corresponding path tracking control methods based on PID control, optimal control, pure tracking control, model predictive control (MPC) or fuzzy control, etc.

[5–8]. The PID control method can eliminate the navigation path tracking deviation, but the PID parameters are difficult to adjust; it requires a certain amount of experience and a large number of parameter tuning tests [9]. The optimal control method simplifies the controlled object as a linear time-invariant system, which can obtain high accuracy and stability with an accurate control model and no disturbance. However, the working environment of the transplanter is complex and changeable, and the performance of the optimal control method is greatly affected by external interference [10]. The pure pursuit control (PPC) method realizes the path tracking control by simulating the geometric model of human driving behavior and combining the simplified two-wheel vehicle model. It is easy to realize and has fewer control parameters, but it is difficult to adjust the optimal look-ahead distance adaptively [11, 12]. The MPC method achieves highly accurate control operations with moderate complexity and allows rolling optimization in a finite time domain to improve accuracy, but the method is difficult to reduce the algorithm computation time without compromising performance, resulting in poor real-time performance [13].

Most of the above path tracking control methods need to establish mathematical models, and the accuracy of mathematical models directly affects the accuracy of path tracking. However, due to the complex and changeable paddy environment, it is difficult to obtain an accurate mathematical model. Fuzzy control is to simulate human driving behavior by expert experience without a precise mathematical model, which is suitable for rice transplanter tracking control of rice transplanter operation in complex and changeable paddy field environment. But with the decrease of input deviation, the control precision of fuzzy control decreases [14–16]. Therefore, variable universe fuzzy control (VUFC) is used to overcome the disadvantages of fuzzy control. In VUFC systems, the control accuracy is influenced by the suitability of the contraction–expansion factor.

To obtain the high control accuracy and improve the path tracking accuracy, a path tracking algorithm for rice transplanter based on VUFC and improved beetle antenna search (BAS) algorithm is proposed in this paper, in which VUFC can achieve adaptive adjustment of the fuzzy universe by dynamically adjusting the contraction–expansion factor, and thus improving the tracking accuracy and stability for the rice transplanter. In the optimal VUFC method, the offline database of contraction–expansion factor is output by an offline iterative optimization method. It calculates the optimal value of the parameter by iterative optimization in an offline simulation model which is a BAS algorithm improved by the isolated niching technique and adaptive step size strategy. The offline parameter optimization method based on BAS can avoid the low precision of path tracking due to the poor real-time performance of the algorithm.

2. Materials and methods

2.1. Automatic navigation rice transplanter platform

The Kubota SPU-68C rice transplanter is used as a test platform for navigation path tracking control, which is composed of a Beidou high-precision differential positioning system, a navigation controller, a steering control device, a vehicle attitude sensor, and a speed control device. The modified rice transplanter is shown in Fig. 1. The main parameters of the platform equipment are shown in Table I. The navigation control software is installed in the laptop. The data of the Beidou differential positioning system and inertial guidance system are obtained through the RS232 serial port. The data sampling frequency of the software is set to 5 Hz. The sensor signals are taken as input, and the desired front-wheel turning angle is output as a control signal which is sent to the steering control device to achieve automatic navigation path tracking.

2.2. Kinematic model of rice transplanter

The accuracy of lateral control during navigation path tracking is closely related to the dynamics of the machinery being studied [17]. And factors such as the complexity of the actual environment and unpredictable external disturbances can have an impact on the actual results of path tracking [18]. Hence, the dynamic analysis of automatic navigation machinery is often studied. Mirzaeinejad and Shafei [19]

https://doi.org/10.1017/S0263574723000905 Published online by Cambridge University Press

Table I. *Navigation hardware parameters of test platform.*

Name	Component	Type	Number	Parameter
Beidou differential positioning system	Position receiver	C201	2	±2 cm, ±0.5° (precision)
	Receiving antenna		3	
	Radio communication module		2	
Navigation controller	Host computer PC		1	
	Lower computer STM32		1	
Steering control device	Stepper motor	57HBP56AL-TF8A	1	1.2 Nm (Torque)
	Stepper motor drives	DRN-130-10	1	$i = 1/10$ (Transmission ratio)
	Hollow rotary platform	RW-ARE-232-DDS-10-24-M-6	1	0°–360° (Working range)
	Absolute encoder		1	
Speed control device	Electric push rod	E6B2-CWZ6C	1	12 mm/s (Speed)
	Incremental photoelectric encoder		1	1000 p/r (Resolution)

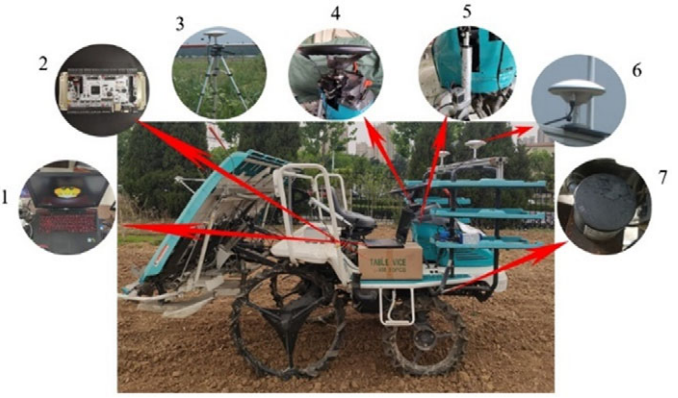

Figure 1. *Test platform for automatic navigation control of rice transplanter. 1. Host computer PC; 2. lower computer STM32; 3. base station; 4. steering control device; 5. speed control device; 6. mobile station antenna; 7. vehicle-angle measurement sensor.*

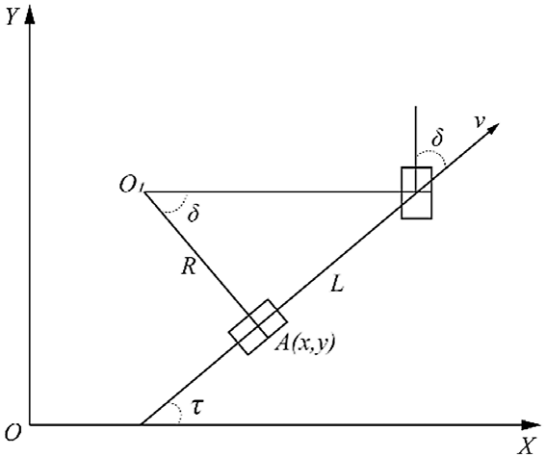

Figure 2. *Schematic diagram of kinematic model of rice transplanter.*

showed in the research that modeling the dynamics of complex working environments is challenging due to the effect of dynamic coupling between the non-holonomic constraint system of the machine and the working environment. Rice is a semi-aquatic plant which is usually cultivated in shallowly flooded conditions. Because of water, the soil surface of a paddy field is uneven, wet, and muddy, which greatly aggravates the difficulty of dynamic analysis for rice transplanters. In view of the difficulty of dynamic analysis and estimation of non-holonomic constraints in complex environments, Shojaei et al. [20] used adaptive robust controllers to estimate the non-holonomic constraints of the upper uncertainty function caused by friction, disturbances, and unmolded dynamics. Considering the incomplete structure of the robot, Azizi and Keighobadi [21] build a discrete kinematic model of the machine. Therefore, the kinematic model of rice transplanter is built for the non-holonomic constraints. The rice transplanter is characterized by low speed and small-angle steering to adjust the driving path during operation. Assuming that the tires are rigid wheels and no lateral forces are generated with the ground, the simplified two-wheeled vehicle kinematic model proposed by Keely is used to build a path tracking simulation model, as shown in Fig. 2 ref. [22].

https://doi.org/10.1017/S0263574723000905 Published online by Cambridge University Press

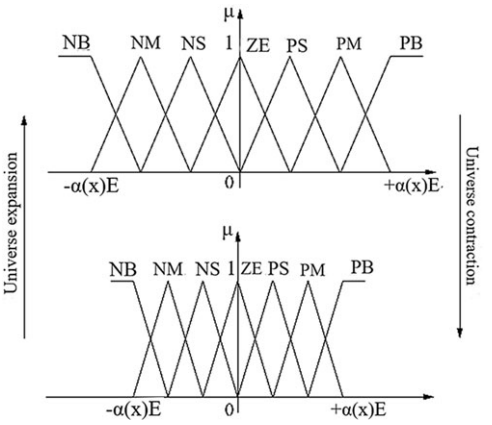

Figure 3. *The variation of variable universes.*

In Fig. 2, point $A(x,y)$ is the rear wheel axis coordinates; L is the wheel distance between the front and rear axles; R is the turning radius; τ is the heading angle; v is the driving speed; and δ is the turning angle of the front wheels. The kinematic model is given by:

$$\dot{x}(t) = v(t)\cos\tau(t) \tag{1}$$

$$\dot{y}(t) = v(t)\sin\tau(t) \tag{2}$$

$$\dot{\tau}(t) = \frac{v(t)\tan\delta(t)}{L} \tag{3}$$

2.3. Basic principles of VUFC algorithm

The performance of fuzzy controller is positively related to the number of fuzzy control rules sets. In traditional fuzzy controllers, the more fuzzy rules there are, the more complex the fuzzy controller becomes, which is difficult to implement. However, fewer fuzzy rules lead to lower control accuracy. In the application of fuzzy controllers, the deviation becomes smaller over time and the number of fuzzy rules applied to becomes less, which leads to a decrease in control accuracy. In the VUFC method, without changing the fuzzy control rules, the universe of the input and output variables is extended and reduced accordingly with the change of the deviation by using the contraction–expansion factor, which is equivalent to adding the fuzzy control rules [23, 24].

Assume that $X_i = [-E_i, +E_i]_{(i=1,2,\ldots,n)}$ and $Y = [-U, +U]$ represent the fundamental universe of input variable $x_{i\,(i=1,2,\ldots,n)}$ and output variable y, respectively. $A = \{A_{ij}\}_{(1\le j\le m)}$ and $B = \{B_j\}_{(1\le j\le m)}$ represent the fuzzy partition on the fuzzy linguistic variables X_i and Y, respectively. Fuzzy inference rules can be formed as follows:

If x_1 is A_{1j}, and x_2 is A_{2j} and. . . and x_n is A_{nj} then y is B_j

The variable universe means that the universes of X_i and Y are varied with the variables x_i and y. The relationships are as follows:

$$X_i(x_i) = [-\alpha_i(x_i)\,E_i, +\alpha_i(x_i)\,E_i] \tag{4}$$

$$Y(y) = \left[-\beta(y)\,U, +\beta(y)\,U\right] \tag{5}$$

where $\alpha_i(x_i)$ and $\beta(y)$ are the contraction–expansion factors of input universe and output universe, respectively. The variation of variable universes is shown in Fig. 3.

As all we known, in the variable domain fuzzy control method, the contraction–expansion factor is a parameter used to promote the domain of the input and output variables to expand accordingly with

https://doi.org/10.1017/S0263574723000905 Published online by Cambridge University Press

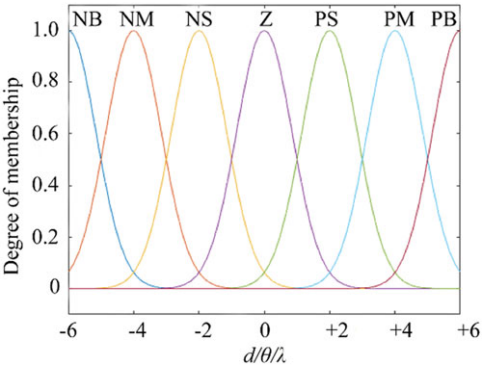

Figure 4. *Gaussian curve affiliation function.*

the change of error, which is equivalent to increasing the fuzzy control rule, thereby improving the accuracy of fuzzy control. Generally, the value range of contraction–expansion factor is set to from 0 to 1 to ensure that the value range of the fuzzy set is within a reasonable range and can be conveniently adjusted with other fuzzy control parameters. In order to ensure that the value range of the fuzzy set is within a reasonable range, the contraction–expansion factors $\alpha_i(x_i)$ and $\beta(y)$ in this work are required to be even functions with the value range [0,1], satisfy the monotonic increasing when $x > 0$.

3. Path tracking control method based on VUFC + improved BAS algorithm

3.1. VUFC design

3.1.1. Fuzzification of input and output variables

The lateral deviation d and heading deviation θ of the transplanter are used as the input variables, and the desired front-wheel turning angle λ of the transplanter is used as the output variable. Specifying lateral deviation d is position when the transplanter is on the right side of the desired path and a negative one on the left side. The heading deviation θ is the angular deviation between the current heading of the transplanter and the desired path of the target point. The direction of the desired path is considered as the starting direction, and the heading deviation θ is defined as counterclockwise positive and clockwise negative.

1. Lateral deviation d. The basic universe is [−0.5 m, +0.5 m], the proportion level is {−6, −4, −2, 0, 2, 4, 6} = {NL, NM, NS, Z, PS, PM, PL}, and the quantization factor is set to12.
2. Heading deviation θ. The basic universe is: [−50°, +50°], the proportion level is {−6, −4, −2, 0, 2, 4, 6} = {NL, NM, NS, Z, PS, PM, PL}, and the quantization factor is set to 0.12.
3. The desired front-wheel turning angle λ. Universe domain is: [−40°, +40°]. The proportion level is {−6, −4, −2, 0, 2, 4, 6} = {NL, NM, NS, Z, PS, PM, PL}, and the scaling factor is set to 6.67.

where {NB, NM, NS, ZE, PS, PM, PB} denote {negative large, negative medium, negative small, zero, positive small, positive medium, positive large}, respectively. The Gaussian curve affiliation function is selected as the affiliation function curve of the above input and output variables, as shown in Fig. 4.

3.1.2. Establishment of fuzzy rules

The position relationship between the rice transplanter and the desired path is shown in Fig. 5. The fuzzy rule table is shown in Table II. The fuzzy rule surface is shown in Fig. 6.

https://doi.org/10.1017/S0263574723000905 Published online by Cambridge University Press

Table II. *Fuzzy control rules.*

The desired front-wheel turning angle λ		Heading deviation θ						
		NB	**NM**	**NS**	**ZE**	**PS**	**PM**	**PB**
Lateral deviation *d*	NB	PS	PS	NM	NB	B	NB	NB
	NM	PM	PS	NS	NM	NM	NM	NM
	NS	PB	PM	ZE	NS	NS	NS	NS
	ZE	PB	PM	PS	ZE	NS	NM	NB
	PS	PS	PS	PS	PS	ZE	NM	NB
	PM	PM	PM	PM	PM	PS	NS	NM
	PB	PB	PB	PB	PB	PM	NS	NS

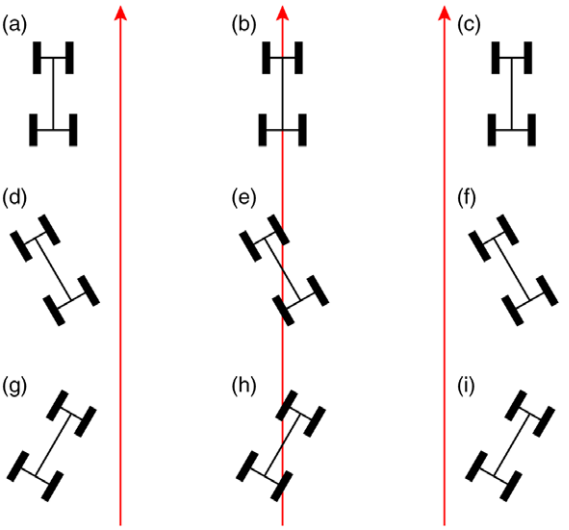

Figure 5. *Position of rice transplanter about desired path.*

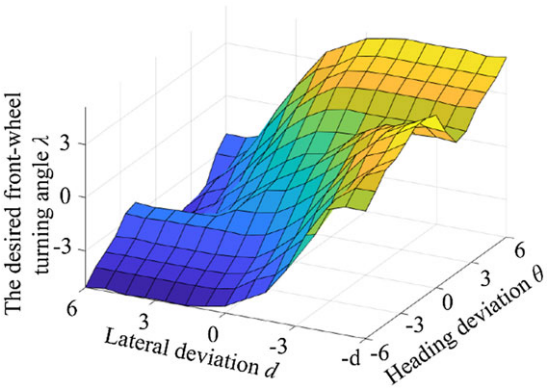

Figure 6. *Fuzzy regular surfaces.*

https://doi.org/10.1017/S0263574723000905 Published online by Cambridge University Press

The rules of fuzzy controller for the desired front-wheel turning angle of rice transplanters are as follows:

1. At conditions (a), (d), and (g), the transplanter is on the left side of the desired path, and the lateral deviation is negatively large (NL). Under conditions (a) and (d), the heading deviations are zero (Z) and positive large (PL), respectively, and the driving direction may be away from the desired path. Therefore, the wheels should turn to the right with a large amplitude, so the desired front-wheel turning angle is negative large (NL). Under condition (g), the heading deviation of the rice transplanter is NL, and the driving direction may be close to the desired path. Therefore, the wheels should turn to the left with a small range, so the desired front-wheel turning angle is positive small (PS).
2. At conditions (b), (e), and (h), the rice transplanter is on the desired path with zero (Z) lateral deviation. In condition (b), the transplanter heading deviation is zero (Z), and the driving direction of the transplanter does not need to be adjusted, so the desired front-wheel turning angle is zero (Z). Under conditions (e) and (h), the heading deviations of the rice transplanter are PL and NL, respectively, and the driving direction of the rice transplanter may tend to be away from the desired path. Under condition (e), the wheels should turn to the right with a larger range, so the desired front-wheel turning angle is NL. Under condition (h), the wheels should turn to the left with a larger range, so the desired front-wheel turning angle is PL.
3. At conditions (c), (i), and (f), the transplanter is on the right side of the desired path, and lateral deviation is PL. Under conditions (c) and (i), the heading deviation of the transplanter is zero (Z) and NL, respectively, and the direction of driving of the transplanter may tend to be away from the desired path, so the wheels should turn to the left with a large range, so the desired front-wheel turning angle is PL. Under the condition (f), the heading deviation of the rice transplanter is PL, and the driving direction tends to be close to the desired path, so the wheels should turn to the right with a small range and the desired front-wheel turning angle is negative small (NS).

3.2. The contraction–expansion factor determination method

Two forms of the contraction–expansion factor function are as follows [25]:

$$\alpha(x) = (|x|/E)^{\tau} + \varepsilon, \tau > 0, \tag{6}$$

$$\alpha(x) = 1 - \omega \exp\left(-kx^2\right), \omega > 0, k > 0. \tag{7}$$

where ε is a sufficiently small positive number.

The contraction–expansion factor in VUFC is usually calculated by a function as in Eqs. (6) and (7). The performance of the VUFC system is influenced by the parameter setting in the functional form, and this parameter setting is not calculated by the formula. This parameter is usually used to derive suitable values using the matching method, but the optimal parameter values are not always derived [26]. The contraction–expansion factor is also usually derived by the second-level fuzzy controller calculation, where the designed fuzzy rule base relies on expert experience [27, 28]. In this study, to solve the above problem of contraction–expansion factor calculation, the BAS algorithm is improved and used to output the optimal contraction–expansion factor.

3.2.1. Principle of BAS algorithm

The BAS algorithm has the advantages of a simple optimization mechanism, convenient implementation, and a small amount of computation, in which a single individual can complete the optimization [29]. But the BAS has the problem that a single individual is easy to fall into local optimization, and the

https://doi.org/10.1017/S0263574723000905 Published online by Cambridge University Press

Algorithm 1 : IABAS algorithm

Input: $f(x)$: the objective function. d: the dimensions of the variables. ub: upper bounds of the variables, where $ub = [ub_1, ub_2, ub_3, \ldots .. ub_d]$. lb: lower bounds of the variables, where $lb = [lb_1, lb_2, lb_3, \ldots .. lb_d]$. n: population size of the beetle. k: number of subpopulations (elite individuals). T: the maximum number of iterations

Output: $x_{\text{best}}, f_{\text{best}}$

1: Initialize a population to get X, Y, iteration number $t = 1$
2: $F_x \leftarrow$ Calculate antennae individual fitness value
3: **while** ($t \leq T$) or (*stop criterion*) **do**
4: E, $F_s \leftarrow$ preserve and update the position and value of the individual with the highest fitness value in the subpopulation
5: **for** p $\leftarrow$ 1 to n **do**
6: $d^t_{o,p,u} \leftarrow$ Calculate distance according to (8)
7: $M \leftarrow$ Calculate step size adjustment factor according to (9)
8: $\text{step}^t_{o,p,u} \leftarrow$ Calculate the step size according to (10)
9: $\boldsymbol{x}^t_{opl}, \boldsymbol{x}^t_{opr} \leftarrow$ Calculate the antennae's positions according to (12)
10: $x^{t+1}_{o,p} \leftarrow$ Update the position of the beetle according to (13)
11: **end for**
12: $F_s \leftarrow$ Calculate average fitness of subpopulations according to (14)
13: $Y \leftarrow$ Calculate subpopulation size according to (15)
14: X, $F_x \leftarrow$ update individual position and Fitness value of beetle population base on Y
15: $t \leftarrow t + 1$
16: **end while**
17: $f_{\text{best}} \leftarrow X_{\text{best}} \leftarrow$ find the position and value of the individual with the highest fitness value in the subpopulation base on $F_{\text{best}}, X_{\text{best}}$
18: **return:** $f_{\text{best}}, X_{\text{best}}$

accuracy is also dependent on the parameter settings [30]. Therefore, we improve the performance of this algorithm from the following aspects:

1. The isolated niching technique is used to avoid getting trapped in a local optimum. The phenomenon of racial segregation resulting from the geographical isolation of nature is referenced as the isolated niche technique. Isolated niche technology is a technology that divides the initial population into multiple subpopulations, and each subpopulation evolves independently. The evolution speed and size of each subpopulation depend on the average adaptation level of each subpopulation [31].
2. The parameter setting problem of the BAS algorithm is solved by using an adaptive step size strategy. When updating, the strategy uses the optimal solution information in the subpopulation to induce the beetle to move to any position between them and the corresponding elite individuals, further improving the search accuracy.

The BAS algorithm based on isolated niche technique and adaptive step size strategy (IABAS) is presented in Algorithm 1. The basic steps are as follows:

Step 1: Set the search space $[lb,ub]$, the number of beetle individuals n, the number of subpopulations k, and the number of iterations T, the dimensions of the variables d. p Individual beetle locations in the search space are generated by uniform distribution and the beetle population location matrix $\mathrm{X} = \begin{bmatrix} x_{11} & \cdots & x_{1d} \\ \vdots & \ddots & \vdots \\ x_{n1} & \cdots & x_{nd} \end{bmatrix}$ is recorded. The search space is divided into a fixed number of subspaces of k, and a subpopulation size matrix $Y = [\, y_1 \ \cdots \ y_k \,]$ is generated. The matrix $F_x = [f_{x_1} \ \cdots f_{x_n}]^T$ of fitness values

https://doi.org/10.1017/S0263574723000905 Published online by Cambridge University Press

corresponding to each individual beetle position, the matrix $F_s = [f_{y_1} \cdots f_{y_k}]^T$ of average fitness in the subspace, the matrix $E = \begin{bmatrix} e_{11} & e_{12} & \cdots & e_{1d} \\ \vdots & & \ddots & \vdots \\ e_{k1} & e_{k2} & \cdots & e_{kd} \end{bmatrix}$ of positions of the elite beetle with the highest fitness value in the subspace, and the fitness value $F_E = [f_{e_1} \cdots f_{e_k}]^T$ of the elite beetle are calculated.

Step 2: Save or update the location and corresponding fitness value of the elite beetle individuals with the highest fitness value in the subspace.

Step 3: When updating the position of each beetle, the distance to the elite beetle individuals in its subpopulation is first calculated. The distance equation for each dimension is as follows:

$$d^t_{o,p,u} = \left| e^t_{o,u} - x^t_{o,p,u} \right| \tag{8}$$

where $d^t_{o,p,u}$ is the uth dimensional position distance between the pth beetle individual and the elite beetle individual in the oth subspace at the tth iteration number. $e^t_{o,u}$ is the uth dimensional position of the elite beetle in the oth subspace at the tth number of iterations. $x^t_{o,p,u}$ is the uth dimensional position of the pth aspen beetle individual in the oth subspace at the tth number of iterations.

Step 4: The step adjustment factor is calculated using a nonlinear function M based on the number of iterations. The function is as follows:

$$\mathrm{M} = (1/t_{\max}) * \exp\left(- \left(\frac{t}{t_{\max}} \right) \right) \tag{9}$$

where $t_{\max}$ is the maximum number of iterations, and t is the current number of iterations. The formula for each dimensional step is as follows:

$$\mathrm{step}^t_{o,p,u} = (1/t_{\max}) * \exp\left(- \left(\frac{\mathrm{t}}{t_{\max}} \right) \right) * d^t_{o,p,u} * \vec{b} \tag{10}$$

where $\mathrm{step}^t_{o,p,u}$ is the uth dimensional step size of the pth beetle individual in the oth subspace at the tth number of iterations, and $\vec{b}$ is the direction of the randomly generated step. $\vec{b}$ is as follows:

$$\vec{b} = \frac{rnd(d, 1)}{\| rnd(d, 1) \|} \tag{11}$$

where $rnd(\cdot)$ is a random function and the resulting number is within $[-1,+1]$, and d is the dimension of the variable.

Step 5: The coordinates of the spatial positions of the left and right antennae of the individual beetle are calculated. The spatial position coordinates are defined as:

$$\begin{cases} \boldsymbol{x}^t_{opl} = \boldsymbol{x}^t_{op} + \mathrm{step}^t_{op} \\ \boldsymbol{x}^t_{opr} = \boldsymbol{x}^t_{op} - \mathrm{step}^t_{op} \end{cases} \tag{12}$$

where $\boldsymbol{x}^t_{op}$ is the position of the pth beetle in the oth subspace under the tth iteration; step^t_{op} is the antenna length of the pth beetle in the oth subspace under the condition of the tth iteration; and $\boldsymbol{x}^t_{opl}$ and $\boldsymbol{x}^t_{opr}$ are the left and right antenna positions of the pth beetle in the oth subspace under the tth iteration, respectively.

If the update position of the left and right antennas of the beetle antenna is outside the position range of the subspace where it is located, the out-of-range update position is cleared.

Step 6: Update the location of the next beetle movement. The formula is defined as:

$$\begin{cases} f^{t+1}_{x_{o,p}} = \min\left(f\left(x^t_{opl} \right), f\left(x^t_{opr} \right) \right) \\ x^{t+1}_{o,p} = \arg\min\limits_{x_{o,p}} f^{t+1}_{x_{o,p}} \end{cases} \tag{13}$$

where $f(x^t_{opl})$ and $f(x^t_{opr})$ are the fitness values at the position of the pth antenna on the left and right side of the antenna in the oth subspace under the tth iteration, respectively. The above equation indicates that the antenna location with the better fitness value is directly selected as the new beetle location.

https://doi.org/10.1017/S0263574723000905 Published online by Cambridge University Press

Step 7: After all beetle positions are updated, the average fitness value F_s is calculated for each subspace. Its calculation formula is as follows:

$$f_{y_o}^t = \frac{\sum_{o=1}^{y_k^t} f_{x_o}^t}{y_o^t} \tag{14}$$

The size Y of each subspace at the next iteration is calculated based on the average fitness value F_s. Its calculation formula is as follows:

$$y_o^{t+1} = n \cdot \frac{f_{y_o}^t}{\sum_{o=1}^{K} f_{y_o}^t} \tag{15}$$

where y_o^{t+1} is the size of the oth subspace at the $t+1$th number of iterations, and $f_{y_o}^t$ is the average fitness value of the other subspace at the tth number of iterations.

Step 8: The number of iterations is updated, and after all the iterations are completed or the termination loop condition is reached, the location information of the optimal fitness value is found in the subspace elite individuals and returned.

3.2.2. Design of fitness function

The search accuracy and convergence speed of the algorithm are directly affected by the selection of the fitness function. In the field of control, time multiplied by integral time absolute error (ITAE) or root mean square error is often used as an indicator to evaluate the performance of control systems. The sum of the ITAE of the obtained lateral deviations and heading deviations is used as a performance index function, which is defined in Eq. (16).

$$f = \varphi \int_0^\infty t|x(t)|dt + (1-\varphi)\int_0^\infty t|y(t)|dt \tag{16}$$

where $x(t)$ is the lateral deviation at time t; $y(t)$ is the heading deviation at time t; and φ is the weight of the ITAE index of lateral deviation in the fitness function.

To improve the reliability of the algorithm, Eq. (16) is simplified as follows:

$$f = \varphi T \sum_{j=0}^{k} t|x(j)| + (1-\varphi)T \sum_{j=0}^{k} t|y(j)| \tag{17}$$

$$t = kT, k = 0, 1, 2, 3 \ldots$$

where T is the system operation period; and k is the number of system calculations.

In the BAS algorithm, the smaller the fitness value, the better the system performance [32]. Hence, the inverse of the performance index function is used as the fitness function as shown in Eq. (18).

$$F = \frac{1}{f} \tag{18}$$

3.2.3. Performance comparison test of IABAS algorithm

To validate the optimization-seeking accuracy of the IABAS algorithm, three benchmark test functions of CEC were selected to test the performance of the IABAS algorithm compared with the BAS algorithm. The expressions formula, dimensions, search ranges, and theoretical optimal value of the used benchmark test functions are shown in Table III.

The IABAS algorithm sets the number of individual beetles to 30, the number of subpopulations to 3, and the number of iterations is set to 500. The BAS algorithm parameters are the same as the above settings. The results are shown in Table IV. The results show that the solution accuracy of the IABAS algorithm is higher than that of the BAS algorithm, and it has good stability and robustness.

https://doi.org/10.1017/S0263574723000905 Published online by Cambridge University Press

Table III. *The benchmark test function.*

Expression formula	Dimensions	Search ranges	Theoretical optimal value
$f_1(x) = \sum_{i=1}^{n} x_i^2$	10	[−100, 100]	0
$f_2(x) = \sum_{i=1}^{n} (x_i + 0.5)^2$	10	[−100, 100]	0
$f_3(x) = -\sum_{i=1}^{n} x_i \sin(\sqrt{\lvert x_i \rvert})$	10	[−100, 100]	−418.9829n

Table IV. *Results of performance comparison tests.*

Method	The benchmark test function	Min	Max	Mean	Std
BAS	$f_1(x)$	4.30E-24	5.70E + 02	1.22E + 02	1.63E + 02
	$f_2(x)$	2.39E-23	6.22E + 02	2.44E + 02	2.95E + 05
	$f_3(x)$	7.31E + 02	8.39E + 02	8.21E + 02	3.35E + 01
Mean value		2.44E + 02	6.77E + 02	3.96E + 02	9.84E + 04
IABAS	$f_1(x)$	9.21E-20	6.80E-01	1.25E-01	2.26E-01
	$f_2(x)$	2.08E-15	7.51E-01	6.83E-02	2.16E-01
	$f_3(x)$	3.72E-13	1.24E + 03	2.49E + 02	4.57E + 02
Mean value		1.25E-13	4.15E + 02	8.31E + 01	1.53E + 02

3.2.4. Offline optimization of the contraction–expansion factor

Offline parameter optimization methods usually do not require real-time processing of data streams and only use the offline method to search parameters comprehensively to find the best parameter combination, which can reduce the running time of path tracking algorithm, so as to avoid the low precision of path tracking due to the poor real-time performance of the algorithm. Hence, to improve the real-time performance of the path tracking control method, an offline parameter optimization method is used to reduce the running time of the algorithm. The problem of low path tracking accuracy caused by the poor real-time performance of the algorithm can be avoided by the offline parameter optimization method. In the initialization of the IABAS algorithm, the search space [*lb*, *ub*] is set to [0, 1], the search dimension d is 2, the number of aspen individuals n is 30, the number of subspaces k is 3, and the number of iterations is 200. The contraction–expansion factor is required to satisfy the property of parity. Therefore, the condition combination of lateral deviation [−0.5 m, +0.5 m] and heading deviation [−50°, +50°] is limited to lateral deviation [0, +0.5 m] and heading deviation [0, 50°]. Multiple combinations of conditions are set under the range of lateral deviation and heading deviation. Offline optimization of parameters is performed afterwards. The basic process of the method for offline optimization of parameters is shown in Fig. 7. Finally, according to the principle of parity, the obtained contraction–expansion factors α and β are extended to the whole lateral deviation and heading deviation, and a base of offline contraction–expansion factors is established. The results of the contraction–expansion factors α and β are shown in Figs. 8 and 9. From Figs. 8 to 9, it can be found that the contraction–expansion factors α and β are real values ranging from 0 to 1, which meet the definition of contraction–expansion factor in variable domain fuzzy control and satisfy the requirements of zero avoidance, monotonicity, coordination, and regularity. The combination of contraction–expansion factors increases gradually when the lateral deviation and heading deviation conditions gradually increase, which ensures the fuzzy domain of the fuzzy control system increases with the increase of contraction–expansion factors, and thus improving the control performance.

https://doi.org/10.1017/S0263574723000905 Published online by Cambridge University Press

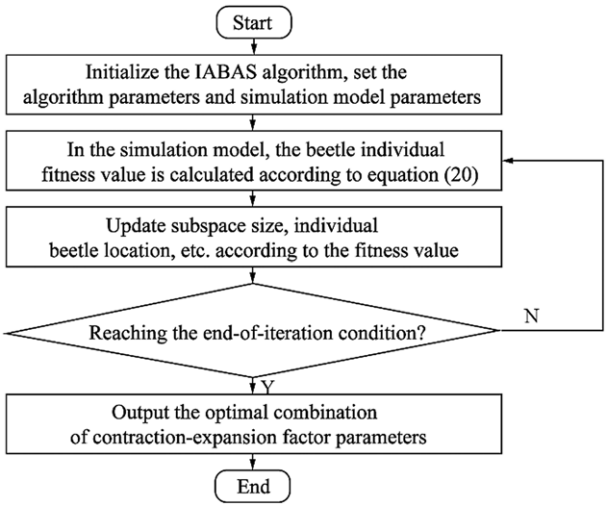

Figure 7. *The basic process of the method for offline optimization of parameters.*

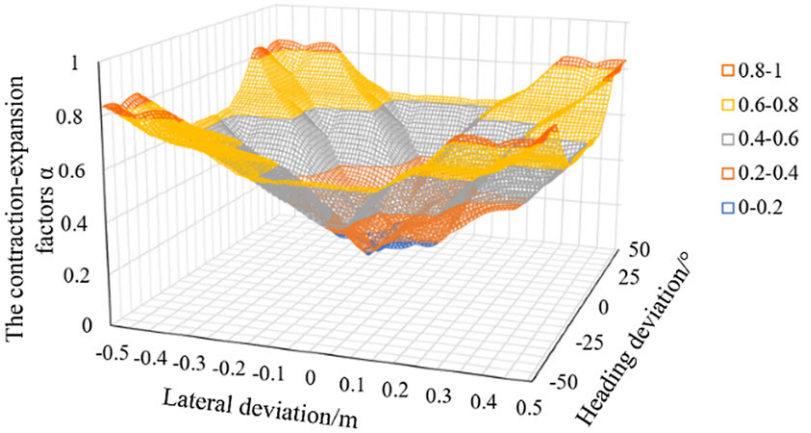

Figure 8. *The optimal contraction–expansion factor α.*

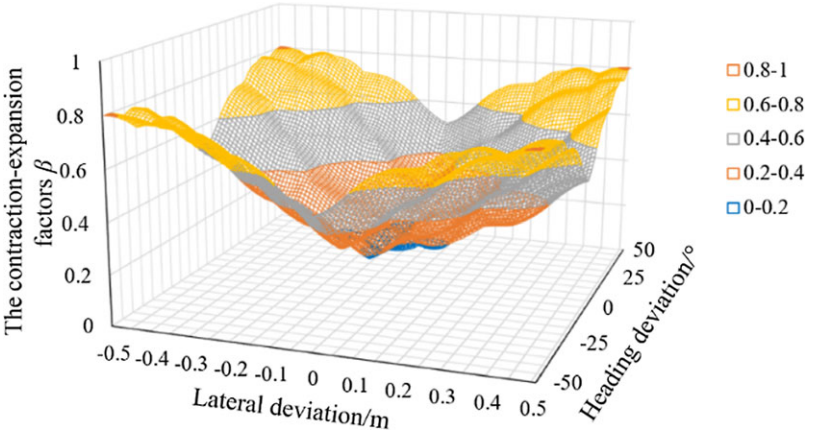

Figure 9. *The optimal contraction–expansion factor β.*

https://doi.org/10.1017/S0263574723000905 Published online by Cambridge University Press

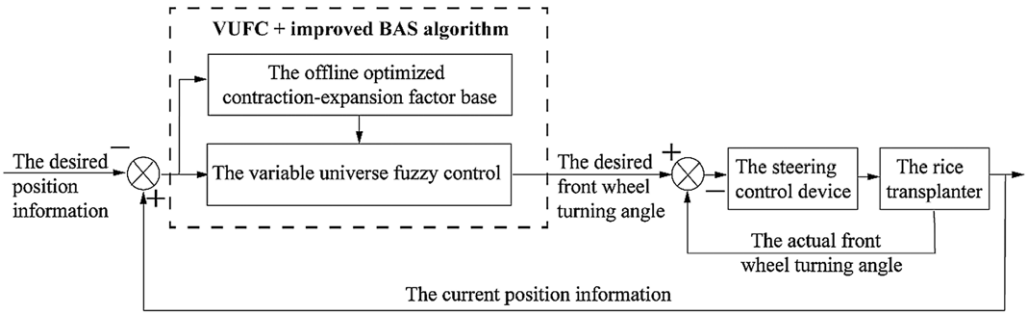

Figure 10. *Block diagram of path tracking control.*

3.3. Structure of the proposed path tracking control method

In summary, a block diagram of path tracking control is shown in Fig. 10. The current position information of the transplanter is obtained by Beidou high-precision differential positioning system. The relative position information is calculated by comparing the current path information with the desired position in the path planning. The optimal contraction–expansion factor parameter combinations are matched by the navigation controller based on relative position information in an offline optimized contraction–expansion factor base. The desired front-wheel turning angle is calculated by the navigation controller based on the obtained contraction–expansion factor with the designed fuzzy rules. The actual front-wheel turning angle is obtained by an absolute encoder in the steering control device. The relative steering angle is obtained by comparing the desired front-wheel steering angle with the actual front-wheel steering angle. The steering control device is used to control the front wheel turning of the rice transplanter according to the obtained relative front-wheel turning angle. Finally, automatic navigation path tracking for rice transplanters is implemented.

3.4. Simulation experiment

To verify the path tracking performance of optimal VUFC, a simulation model in MATLAB/Simulink is built. The performance of the algorithm is first verified using S-shaped paths and compared with the traditional variable domain fuzzy control algorithm for path tracking performance, where the S-shaped paths contain two straight-line paths and one curved path, and the curved path uses a semicircular turn. In addition, in the simulation, three different initial values of lateral deviation (0.2, 0.4, and 0.6 m) are chosen, while setting the heading deviation to 0, and three driving speeds (0.4, 0.8, and 1.2 m/s) are tested. The simulations were conducted in a total of 3×3 sets of experiments. The lateral deviation is used as an important indicator of the operational accuracy of the rice transplanter, so a specific analysis of the lateral deviation is performed. The lateral deviation during path tracking is generally within ± 5 cm as the entering steady state of path tracking. The time of entering steady state of path tracking is used as the adjustment time t_s (s). The overshoot Mp (m) is used as an indicator to assess the relative stability of the system. Adjustment time t_s (s) and rise time t_r (s) are used as indicators to assess the rapidity of the system.

The simulation results are shown in Figs. 11 and 12. Compared with the variable domain fuzzy control before optimization, the optimized variable domain fuzzy control can make the simulated trajectory of the vehicle closer to the planned path. The lateral deviation in the ground head turn is also lower, and the maximum lateral deviation is 0.164 m. When the transplanter passes through the ground head turn, the transplanter can enter the linear path tracking state well. After entering the linear path working area, the path tracing performance of the optimized variable domain fuzzy control is better than that of the

https://doi.org/10.1017/S0263574723000905 Published online by Cambridge University Press

Table V. *Results of the simulation experiment.*

Method	Initial lateral deviation (m)	$V = 0.40$ m/s			$V = 0.80$ m/s			$V = 1.20$ m/s		
		Mp (m)	t_r (s)	t_s (s)	*Mp* (m)	t_r (s)	t_s (s)	*Mp* (m)	t_r (s)	t_s (s)
The proposed	0.20	0	5.00	5.80	0	2.60	3.00	0	1.40	2.20
method	0.40	0	6.60	8.60	0	3.20	4.40	0	2.00	2.80
	0.60	0	7.60	11.20	0	3.80	5.60	0	2.80	3.80
Mean value		0	6.40	8.53	0	3.2	4.33	0	2.06	2.93

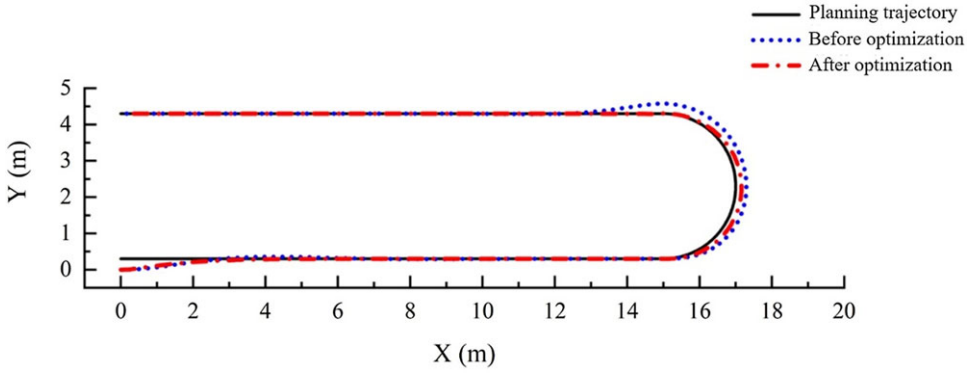

Figure 11. *Simulation trajectory comparison.*

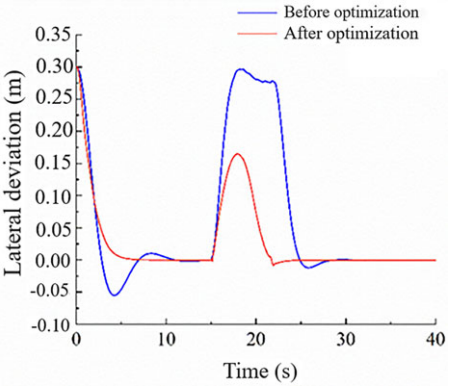

Figure 12. *Lateral deviation comparison.*

variable domain fuzzy control before optimization. Besides, overshoot and time to stabilize are used as quantitative comparison indicators as shown in Table V. In the case of constant initial lateral deviation, the initial lateral deviation is within 0.60 m, the optimal VUFC path tracking overshoot *Mp* is 0, the average time to enter the path tracking steady state is less than 8.53 s, and the rise time t_s is less than 6.40 s. The results show that the proposed algorithm has a small amount of overshoot and the time to enter the steady state of path tracking.

https://doi.org/10.1017/S0263574723000905 Published online by Cambridge University Press

Figure 13. *The field experiment of automatic operation of rice transplanter.*

4. Field experiment and discussion

4.1. Field experiment

To verify the performance of the proposed path tracking control method, a linear path tracking comparison experiment in the paddy field is performed by comparing it with the PPC method. The field experiment is conducted at the Guohe Experimental Base of the Anhui Agricultural University. The depth of the paddy soil is approximately 20 cm. The field experiment for the automatic navigation of the rice transplanter is shown in Fig. 13. In the field experiment, a marked path is planned in advance with two ends set at points A and B, which was used as the linear desired path for the rice transplanter path tracking. Driving the rice transplanter artificially is slowly along the marked path. During this process, the positioning information of the transplanter is recorded by the GPS, and the navigation coordinate points are fit into a path in the host computer, which is used as the linear desired path for the rice transplanter path tracking. Then, the initial heading deviation of the transplanter is adjusted to 0°, and the transplanter moves to the starting position of the linear desired path and begins to move the path until the end in the automatic navigation model. The information of parameters including position and attitude of the transplanter is recorded in real-time when it moves automatically, where the system sampling frequency is set to 5 Hz and the sampling time is set to 50 s. In the pure pursuit algorithm, the look-ahead distance is set to 1.2 m.

4.2. Analysis of field experiment results

The experimental results are analyzed using the overshoot Mp (m), the rise time t_r (s), the adjustment time t_s (s), and absolute mean steady-state error $|e_s|$ (m), and the comparison results are shown in Tables VI–VIII. It can be found that, with constant initial lateral deviation, the values of overshoot Mp and absolute mean steady-state error $|e_s|$ are increased, while the values of rise time t_r (s) and adjustment time t_s are decreased as the driving speed of the transplanter increases. In addition, compared with the pure pursuit algorithm, the optimized variable domain fuzzy control algorithm can reduce the overshoot by 0.039, 0.031, and 0.039 m, the rise time t_r by 5.2, 2, and 0.3 s, the adjustment time t_s (s) by 5.2, 2.9, and 1.4 s, and the absolute mean error $|e_s|$ by 0.003, 0.003, and 0.004 m, respectively. As shown in Tables VI–VIII, the optimal variable domain fuzzy control algorithm proposed in this work can reduce the overshoot and stabilization time.

In addition, the curves of the algorithm performance comparison are given in Fig. 14. From Fig. 14, it can be seen that under different initial lateral deviation condition, the proposed algorithm has smaller path tracking response time and can quickly eliminate lateral deviations compared with the PPC method. Figure 15 shows box plots of the algorithm performance comparison. As shown in Fig. 15, the overshoot, rise time, adjustment time, and absolute average steady-state error of the proposed time are smaller than

https://doi.org/10.1017/S0263574723000905 Published online by Cambridge University Press

Table VI. *Comparison results of path tracking performance at a driving speed of 0.4 m/s.*

Method	Initial lateral deviation (m)	$V = 0.4$ m/s			
		Mp **(m)**	t_r **(s)**	t_s **(s)**	$\lvert e_s \rvert$ **(m)**
The proposed method	0.2	0.021	5.2	6.2	0.011
	0.4	0.011	7.6	9.0	0.010
	0.6	0.010	8.0	12.4	0.009
Mean value		0.014	6.9	9.2	0.010
The pure pursuit control method	0.2	0.052	6.6	10.0	0.012
	0.4	0.059	12.6	14.4	0.011
	0.6	0.048	17.6	18.8	0.013
Mean value		0.053	12.3	14.4	0.012

Table VII. *Comparison results of path tracking performance at a driving speed of 0.8 m/s.*

Method	Initial lateral deviation (m)	$V = 0.8$ m/s			
		Mp **(m)**	t_r **(s)**	t_s **(s)**	$\lvert e_s \rvert$ **(m)**
The proposed method	0.2	0.037	2.8	3.2	0.018
	0.4	0.031	3.4	4.8	0.020
	0.6	0.034	5.6	7.2	0.019
Mean value		0.034	3.9	5.1	0.019
The pure pursuit control method	0.2	0.062	5.0	5.2	0.022
	0.4	0.072	5.4	8.8	0.020
	0.6	0.061	7.2	10.0	0.025
Mean value		0.065	5.9	8.0	0.022

Table VIII. *Comparison results of path tracking performance at a driving speed of 1.2 m/s.*

Method	Initial lateral deviation (m)	$V = 1.2$ m/s			
		Mp **(m)**	t_r **(s)**	t_s **(s)**	$\lvert e_s \rvert$ **(m)**
The proposed method	0.2	0.044	1.8	2.0	0.026
	0.4	0.040	2.2	3.2	0.029
	0.6	0.042	5.6	6.8	0.032
Mean value		0.042	3.2	4.0	0.029
The pure pursuit control method	0.2	0.056	3.2	4.0	0.036
	0.4	0.078	3.8	5.2	0.034
	0.6	0.140	3.4	7.0	0.031
Mean value		0.091	3.5	5.4	0.033

those of the PPC method. And the distance between the upper quartile and the lower quartile is also smaller than that of pure tracking, indicating that the data of the proposed method are more concentrated and the proposed method has better straight-line path tracking performance. In general, the comparative test shows that fast and stable entry of the linear tracking state performance can be obtained by adjusting the fuzzy universe with VUFC and selecting the combination of contraction–expansion factors in the offline database of contraction–expansion factor by looking up the table according to the lateral deviation and heading deviation.

https://doi.org/10.1017/S0263574723000905 Published online by Cambridge University Press

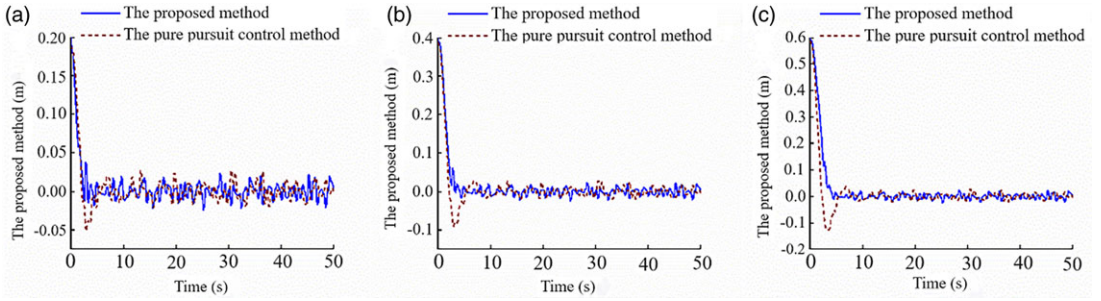

Figure 14. *Curves of algorithm performance comparison. (a) The initial deviation is 0.2 m. (b) The initial deviation is 0.4 m. (c) The initial deviation is 0.6.*

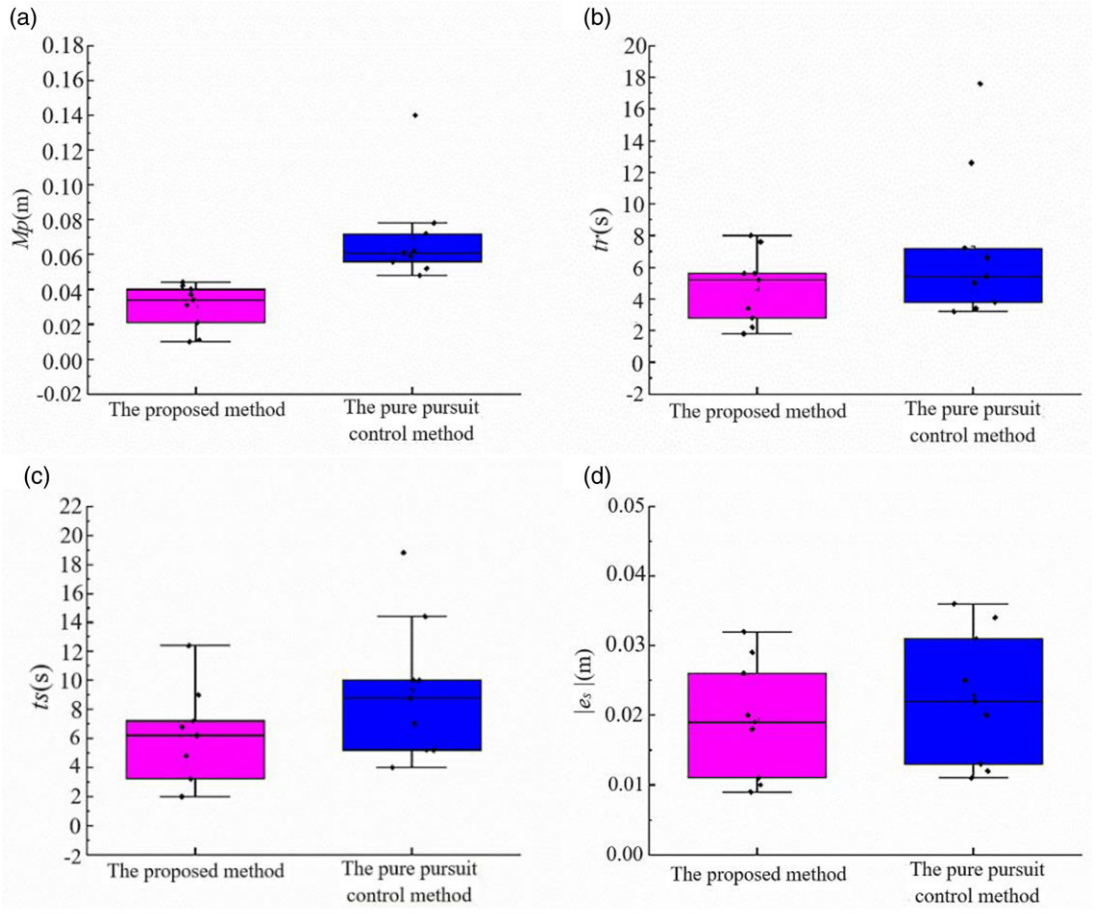

Figure 15. *Box plot of algorithm performance comparison. (a) Overshoot Mp (m). (b) Rise time t_r (s). (c) Adjustment time t_s (s). (d) Absolute average steady-state error $|e_s|$ (m).*

4.3. Comparative analysis with the results of existing studies

Comparing with existing studies, Yin et al. [33] proposed a path tracking algorithm based on speed-adaptive fuzzy control for rice transplanter. The comparison results are shown in Table IX. The distance of entering steady state of path tracking of this paper is calculated by the product of the time of entering

https://doi.org/10.1017/S0263574723000905 Published online by Cambridge University Press

Table IX. *The results of the proposed method compared with Yin et al.*

Method	Speed (m/s)	Initial lateral deviation (m)	*Mp* (m)	The distance of entering steady state of path tracking (m)
Yin et al.	0.3 m/s	0.250	0.125	> 20
The proposed method	0.4 m/s	0.200	0.021 (83%↓)	2.48 (87%↓)
Yin et al.	1.3 m/s	0.250	0.080	> 20
The proposed method	1.2 m/s	0.200	0.044 (45%↓)	2.40 (88%↓)
Yin et al.	Variable speed	0.250	0.075	13.00
The proposed method	Average speed	0.200	0.034 (54%↓)	2.48 (80%↓)

steady state of path tracking (t_s) and the speed (v). The results of this paper under average speed conditions are obtained by calculating the average values of Mp and t_s at three different driving speeds of 0.4, 0.8, and 1.2 m/s.

In Table IX, the results are compared with approximately the same initial conditions. Under low speed conditions, the Mp of the proposed method in this paper is 83% lower than that of Yin et al., and the distance of entering steady state of path tracking of this paper is at least 87% lower than that of Yin et al. Under high speed conditions, the Mp of the proposed method in this paper is 45% lower than that of Yin et al. and the distance of entering steady state of path tracking of this paper is at least 88% lower than that of Yin et al. Comparing the average speed results of this paper with the variable speed results of Yin et al., the Mp of the proposed method in this manuscript is 54% lower than that of Yin et al., and the distance of entering steady state of path-tracking of this paper is 80% lower than that of Yin et al. Part of the reason for the poorer comparison results of Yin et al is that the tracking paths include curved paths. Overall, the effect of path tracking can be influenced by driving speed during linear path tracking, but the proposed method can effectively reduce the time of entering steady state of path tracking. Under the same deviation condition, the proposed method can achieve better path tracking accuracy at different driving speeds.

5. Conclusion

This study provides a path tracking control method based on VUFC and improved BAS algorithm for rice transplanter in which VUFC is used for path tracking control and BAS is applied to obtain the contraction–expansion factor in VUFC.

In the method, VUFC can achieve adaptive adjustment of the fuzzy universe by dynamically adjusting the contraction–expansion factor in the complex paddy field environments, and an offline parameter optimization method based on BAS is used to build the offline database of contraction–expansion factor. In the paddy field application, an automated rice transplanter has low traction and is prone to sideslip and bump when it moves across an uneven and muddy paddy field, which can cause large fluctuation of the attitude of the transplanter. However, the combination of contraction–expansion factors can be obtained in the offline database of contraction–expansion factor by looking up the table according to the lateral deviation and heading deviation. Setting the contraction–expansion factor of VUFC in variable environments can effectively reduce the time of entering steady state of path tracking and improve the path tracking accuracy and efficiency of rice transplanter.

The automatic steering experimental platform is modified and used to perform simulations and experiments to verify the effectiveness of the proposed method. Experimental results demonstrate that the proposed method can reduce the time of entering the stable state of linear path tracking and achieve the accuracy and stability of path tracking compared with the PPC method. The method in this study still has limitations. The accuracy of the path tracking simulation model can affect the performance of the offline parameter optimization method. In the future research work, a path tracking simulation model will be

https://doi.org/10.1017/S0263574723000905 Published online by Cambridge University Press

further optimized to be more consistent with the actual paddy field environment through modeling the tire-soil pavement interaction force.

Author's contribution. Dequan Zhu: Conceptualization, methodology, and software. Menghao Shi: Data curation and writing – original draft preparation. Yang Wang and Kang Xue: Visualization, investigation, and validation. Juan Liao and Wei Xiong: Supervision. Fuming Kuang and Shun Zhang: Writing – reviewing and editing.

Financial support. This work was funded by the Natural Science Foundation of Anhui Province (Grant No. 2208085ME131), the National Natural Science Foundation of China (Grant No.32201665), the Nature Science Research Project of Anhui province (Grant Nos. 2108085MC96), and Key Common Technology Research and Development Projects in Hefei (Grant No. 2021GJ078).

Competing interests. The authors declare none.

Ethical approval. Not applicable.

References

[1] J. Hu, L. Gao and X. Bai, "Review of research on automatic guidance of agricultural vehicles," *Trans. CSAE* **31**(10), 1–10 (2015).
[2] C. Ji and J. Zhou, "Current situation of navigation technologies for agricultural machinery," *Trans. CSAM* **45**(9), 44–54 (2014).
[3] H. Wang, G. Wang and X. Luo, "Path tracking control method of agricultural machine navigation based on aiming pursuit model," *Trans. CSAE* **35**(4), 11–19 (2019).
[4] W. Zhang, J. Gai, Z. Zhang, L. Tang, Q. Liao and Y. Ding, "Double-DQN based path smoothing and tracking control method for robotic vehicle navigation," *Comput. Electron. Agric.* **166**, 104985 (2019).
[5] S. De, R. Tabile, R. Inamasu and A. Porto, "A row crop following behavior based on primitive fuzzy behaviors for navigation system of agricultural robots," *IFAC-Proc.* **46**(18), 91–96 (2013).
[6] Z. He, L. Nie, Z. Yin and S. Huang, "A two-layer controller for lateral path tracking control of autonomous vehicles," *Sensors (Basel)* **20**(13), 3689 (2020).
[7] S. Moveh, H. Mohamed and M. Binti, "A review of some pure-pursuit based path tracking techniques for control of autonomous vehicle," *Int. J. Comput. Appl.* **135**(1), 35–38 (2016).
[8] X. Yin, J. Du, D. Geng and C. Jin, "Development of an automatically guided rice transplanter using RTK-GNSS and IMU," *IFAC-PapersOnLine* **51**(17), 374–378 (2018).
[9] X. Luo, Z. Zhang and Z. Zhao, "Design of DGPS navigation control system for Dongfanghong X-804 tractor," *Trans. CSAE* **25**(11), 139–145 (2009).
[10] J. Chen, C. Niao and Z. Zhu, "Study on automatic guidance for tractor on grassland," *Trans CSAM* **36**(7), 104–107 (2015).
[11] P. Huang, Z. Zhang, X. Luo and P. Huang, "Path tracking control of a differential-drive tracked robot based on look-ahead distance," *IFAC-PapersOnLine* **51**(17), 112–117 (2018).
[12] B. Mehmet, K. Ehsan and H. Hasan, "Double look-ahead reference point control for autonomous agricultural vehicles," *Biosyst. Eng.* **113**(2), 173–186 (2012).
[13] Y. Ding, L. Wang, Y. Li and D. Li, "Model predictive control and its application in agriculture: A review," *Comput. Electron. Agric.* **151**, 104–117 (2018).
[14] T. Hamid and R. Subhash, "Path-tracking of autonomous vehicles using a novel adaptive robust exponential-like-sliding-mode fuzzy type-2 neural network controller," *Mech. Syst. Signal Process.* **130**, 41–55 (2019).
[15] S. Li, H. Xu, Y. Ji, R. Cao, M. Zhang and H. Li, "Development of a following agricultural machinery automatic navigation system," *Comput. Electron. Agric.* **158**, 335–344 (2019).
[16] Q. Meng, R. Qiu, J. He, M. Zhang, X. Ma and G. Liu, "Development of agricultural implement system based on machine vision and fuzzy control," *Comput. Electron. Agric.* **112**, 128–138 (2015).
[17] M. H. Korayem, S. R. Nekoo and S. Kazemi, "Finite-time feedback linearization (FTFL) controller considering optimal gains on mobile mechanical manipulators," *J. Intell. Robotic Syst.* **94**(3–4), 1–18 (2019).
[18] S. A. A. M. Keymasi Khalaji, "Adaptive sliding mode control of a wheeled mobile robot towing a trailer," *Proc. Inst. Mech. Eng., Part I: J. Syst. Control Eng.* **229**(2), 169–183 (2015).
[19] H. Mirzaeinejad and A. M. Shafei, "A novel recursive formulation for dynamic modeling and trajectory tracking control of multi-rigid-link robotic manipulators mounted on a mobile platform," *Proc. Inst. Mech. Eng., Part I: J. Syst. Control Eng.* **235** (7), 1204–1217 (2021).
[20] K. Shojaei, A. R. M. Shahri and A. R. Tarakameh, "Adaptive feedback linearizing control of nonholonomic wheeled mobile robots in presence of parametric and nonparametric uncertainties," *Robot. Comput. Integr. Manuf.* **27**(1), 149–204 (2011).
[21] M. R. Azizi and J. Keighobadi, "Point stabilization of nonholonomic spherical mobile robot using nonlinear model predictive control," *Robot. Auton. Syst.* **98**, 347–359 (2017).
[22] A. Keely, *A Feedforward Control Approach to the Local Navigation Problem for Autonomous Vehicles* (Carnegie Mellon University, USA, 1994).

[23] J. Liu, X. Li and Y. Zang, "Modelling and experimental study on active energy-regenerative suspension structure with variable universe fuzzy PD control," *Shock Vib.* **2016**, 1–11 (2016).
[24] J. Zheng, J. Chen and O. Quan, "Variable universe fuzzy control for battery equalization," *J. Syst. Sci. Complex.* **31**(1), 325–342 (2018).
[25] H. Pang, F. Liu and Z. Xu, "Variable universe fuzzy control for vehicle semi-active suspension system with MR damper combining fuzzy neural network and particle swarm optimization," *Neurocomputing* **306**, 130–140 (2018).
[26] Y. Wang, M. Wei, X. Hu, M. Jang and L. Zhang, "Research on variable universe fuzzy PID control strategy of pipe lining induction heating system," *Model. Simul. Eng.* **2020**, 1–9 (2020).
[27] G. Ma, Z. Yu, G. Cao, R. Zhang and Y. Zheng, "The motion path study of measuring robot based on variable universe fuzzy control," *MATEC Web Conf.* **95**, 8011 (2017).
[28] J. Yao, J. Lu and Y. Zheng, "DC motor speed control of annual-ring measuring instrument based on variable universe fuzzy control algorithm," *Trans. CSAE* **35**(14), 57–63 (2019).
[29] X. Jiang and S. Li, "BAS: Beetle antennae search algorithm for optimization problems," *Int. J. Robot. Control* **1**(1), 1–5 (2018).
[30] Y. Fan, J. Shao, G. Sun and X. Shao, "Improved beetle antennae search algorithm-based Lévy flight for tuning of PID controller in force control system," *Math. Probl. Eng.* **2020**, 1–22 (2020).
[31] Y. Lin, J. Hao and Z. Ji, "A study of genetic algorithm based on isolation niche technique," *J. Syst. Eng.* **15**(1), 86–91 (2000).
[32] X.-L. Li, R. Serra, J. Olivier and C. Fei, "Performance of fitness functions based on natural frequencies in defect detection using the standard PSO-FEM approach," *Shock Vib.* **2021**(1), 1–9 (2021).
[33] J. Yin, D. Zhu, J. Liao, L. Liu, Y. Wang and T. Chu, "Path tracking algorithm based on speed-adaptive fuzzy control for rice transplanter," *Int. Agric. Eng. J.* **28**(4), 1–9 (2019).

Cite this article: D. Zhu, M. Shi, Y. Wang, K. Xue, J. Liao, W. Xiong, F. Kuang and S. Zhang (2023). "Path tracking control method for automatic navigation rice transplanters based on VUFC and improved BAS algorithm", Robotica **41**, 3116–3136. https://doi.org/10.1017/S0263574723000905